# Efficiency of electrical manipulation in two-dimensional topological insulators*

Pang Mi(庞 蜜)† and Wu Xiao-Guang(吴晓光)

*SKLSM, Institute of Semiconductors, Chinese Academy of Sciences, Beijing* 100083, *China*

(Received 14 December 2013; revised manuscript received 22 January 2014; published online 15 May 2014)

We investigate the efficiency of electrical manipulation in a two-dimensional topological insulator by inspecting the electronic states of a lateral electrical potential superlattice in the system. The spatial distribution of the electron density in the system can be tuned by changing the strength of the externally applied lateral electrical superlattice potential. This provides us the information about how efficiently one can manipulate the electron motion inside a two-dimensional topological insulator. Such information is important in designing electronic devices, e.g., an electric field effect transistor made of the topological insulator. The electronic states under various conditions are examined carefully. It is found that the dispersion of the mini-band and the electron distribution in the potential well region both display an oscillatory behavior as the potential strength of the lateral superlattice increases. The probability of finding an electron in the potential well region can be larger or smaller than the average as the potential strength varies. These features can be attributed to the coupled multiple-band nature of the topological insulator. In addition, it is also found that these behaviors are not sensitive to the gap parameter of the two-dimensional topological insulator model. Our study suggests that the electron density manipulation via electrical gating in a two-dimensional topological insulator is less effective and more delicate than that in a traditional single-band semiconductor.

**Keywords:** topological insulator, lateral potential superlattice, electrical manipulation

**PACS:** 73.21.Cd, 73.22.Dj **DOI:** 10.1088/1674-1056/23/7/077302

## 1. Introduction

The topological insulator has received widespread attention in recent years because of its exotic electronic properties, which suggest wonderful prospects both in the fundamental study and for industrial applications.[1–6] Its novel feature lies on the observation that when it is of a finite size, it has linearly dispersive surface states (edge states in the two-dimensional system case) in the bulk gap.[7–10] The robustness of the surface states against disorder scatterings makes the topological insulator a promising new member of materials useful in the future information technology.

In practical electronic device applications, the electrical manipulation of the carrier motion by voltage gates provides a basic and important mechanism for the functioning of the devices. For example, in a CMOS transistor made of the conventional semiconductors, the electron density can be manipulated by gating in such a way that one can control the electrical current through the device. It thus becomes a crucial task to learn how to control the behavior of electrons in the topological insulator by using electric fields. Various researches concerning this issue have been carried out.[11–23] If an edge state can be created by electric voltage gates, i.e., the carriers in the system can be confined/depleted spatially by the electrical potential, it would greatly enhance the utilization of the topological insulator as a building block for the future electronic devices.

The effective model put forward in Ref. [24] has been widely used to describe the two-dimensional (2D) topological insulator.[11–14,18,25–33] In that model, one deals with a coupled two-component system (more generally, when the spin–orbit interaction is considered, it is a four-component system). The model resembles the Dirac equation describing a Dirac fermion, which is known to exhibit the Klein tunneling phenomenon[34] and consequently a potential barrier may not be able to confine the fermion motion spatially. Therefore, it will be interesting and meaningful to examine the influence of a spatially defined potential on the 2D topological insulator, especially the confinement of the electron wave functions by an externally applied electrical potential. The present paper is devoted to this very important problem. We simplify the issue by considering a lateral electrical potential superlattice structure made of a 2D topological insulator with spatially periodic, square shaped, electrical potential barriers created by an electric gate voltage. The single-electron energy dispersion and wave functions are calculated. The spatial dependence of the wave functions is investigated when the lateral superlattice potential is varied.

The paper is organized as follows. In Section 2, the theoretical formulation is presented. Section 3 contains our calculated results and the discussion. Finally, a summary is provided.

*Project supported by the National Natural Science Foundation of China (Grant Nos. 61076092 and 61290303).

†Corresponding author. E-mail: pangmi@semi.ac.cn

© 2014 Chinese Physical Society and IOP Publishing Ltd 

## 2. Formulation and calculation

The 2D topological insulator is modeled by the following well-known Hamiltonian:[24]

$$\begin{pmatrix} h(\boldsymbol{k}) & 0 \\ 0 & h^*(-\boldsymbol{k}) \end{pmatrix}, \tag{1}$$

where $\boldsymbol{k} = (k_x, k_y)$, $h(\boldsymbol{k}) = \varepsilon(\boldsymbol{k}) + \sum_\alpha d_\alpha(\boldsymbol{k})\sigma_\alpha$ with $\sigma_\alpha$ the Pauli matrix, $\varepsilon(\boldsymbol{k}) = C - D(k_x^2 + k_y^2)$, $d_1 = Ak_x$, $d_2 = Ak_y$, and $d_3 = M - B(k_x^2 + k_y^2)$. Here $A$, $B$, $C$, $D$, and $M$ are parameters determined by the structure of the quantum well.[24] The parameter $C$ gives the zero-point energy and in this paper, we can safely set it to zero for simplicity. When there is no coupling between the spins, the lower $2\times 2$ block $h^*(-\boldsymbol{k})$ and the upper block $h(\boldsymbol{k})$ are decoupled. They have the same energy spectrum and the corresponding wave functions are connected via a unitary transformation of the time reversal operator. Thus in this paper, we will limit ourselves to the analysis of the upper block $h(\boldsymbol{k})$.

The topological insulator is in the $xy$ plane, and the lateral potential superlattice is assumed to be along the $x$ axis and uniform in the $y$ direction. The Hamiltonian describing the lateral superlattice is assumed to be $H = h(\boldsymbol{k}) + V(x)$. The potential $V(x)$ is diagonal and periodic in $x$. For simplicity, a square barrier potential is assumed. In one unit cell $x \in [0, L]$, $V(x) = 0$ for $x \in [R/2, L - R/2]$, and $V(x) = V_0$ otherwise, where $L$ is the period of the lateral superlattice and $R$ is the width of the potential barrier in one unit cell. The lateral superlattice could be implemented by periodically depositing metal strips on the surface of a 2D topological insulator with the help of modern lithography technology. The barrier potential height could be varied by adjusting the bias voltage applied to the metal strips. The 2D topological insulator model is derived from a multiple-band envelope function model.[24] Thus, the assumption of a diagonal $V(x)$ is reasonable and consistent with the model. Actually, a similar potential profile has been used in graphene.[35]

The system is translational invariant in the $y$ direction, and $k_y = p_y/\hbar$ is a good quantum number. However, because of the presence of potential $V(x)$, there is no translational invariance in the $x$ direction, and we follow the Peierls substitution to replace $k_x$ in Eq. (1) by the differential operator $-\mathrm{i}\partial_x$. The explicit form of the Hamiltonian thus is

$$H = \begin{pmatrix} M + d_+k^2 + V(x) & Ak_- \\ Ak_+ & -M + d_-k^2 + V(x) \end{pmatrix}, \tag{2}$$

with $d_+ = -(B+D)$, $d_- = B - D$, $k^2 = k_+k_-$, $k_+ = -\mathrm{i}\partial_x + \mathrm{i}k_y$, and $k_- = -\mathrm{i}\partial_x - \mathrm{i}k_y$.

The wave function of the above Hamiltonian can be written as

$$\psi(x,y) = \frac{\mathrm{e}^{\mathrm{i}k_y y}}{\sqrt{L_y}} \mathrm{e}^{\mathrm{i}q_x x} \begin{pmatrix} u^{\mathrm{u}}(x) \\ u^{\mathrm{l}}(x) \end{pmatrix}, \tag{3}$$

with $L_y$ the system size in the $y$ direction and $q_x$ the mini-band wave vector. Here $u^{\mathrm{u}}(x) = u^{\mathrm{u}}(x+L)$ and $u^{\mathrm{l}}(x) = u^{\mathrm{l}}(x+L)$ give the upper and the lower components of the periodic part of the wave function. The wave vector $q_x$ should be limited to the first Brillouin zone $q_x \in [-\pi/L, \pi/L]$. In the present paper, the plane wave expansion approach is used and a sufficient number of plane waves are used to achieve the necessary accuracy for the energy levels. The wave function $u^s(x)$ can be written as $u^s(x) = L^{-1/2}\sum_n c_n^s \mathrm{e}^{\mathrm{i}2\pi nx/L}$, where $s$ stands for u or l. The wave function $u^s(x)$ is normalized to unity in one unit cell.

The model for the 2D topological insulator contains many parameters. In the present paper, we mainly consider the influence of the gap parameter $M$, as its sign has a profound effect on the electronic property when the 2D topological insulator has a finite size.[24,25] The numerical values of other parameters $A$, $B$, and $D$ are taken from Ref. [24]. The influence of the strength of the superlattice potential $V_0$ will also be studied.

## 3. Results and discussion

In the absence of a periodic potential, the bulk 2D topological insulator has approximately two bands.[24] The introduction of the lateral potential superlattice $V(x)$ leads to a multiple-energy band structure. The eigen energy of Hamiltonian $H$ becomes $E_i(q_x, k_y)$ with $i$ the band index. Extensive numerical works have been carried out, and qualitatively the same results were obtained. In the following, we show the calculated results for a typical case of $L = 20$ nm and $R = 0.5123456L$. The ratio $R/L$ is chosen to avoid possible length commensurate artifacts, and other ratios are also used.

It is found that as $V_0$ increases (decreases), each band energy $E_i\ (q_x, k_y)$ increases (decreases) as a whole roughly with an amount of $V_0R/L$, the averaged potential energy in one unit cell. Furthermore, for a given $V_0$, if one takes the averaged potential $V_0R/L$ as the energy zero point, then the $m$-th band above or below this averaged potential energy will approximately have its largest expansion coefficient $|c_n^s|$ at $|n| \sim |m|$ ($n = 0, \pm 1, \pm 2, \ldots$). The $|c_n^s|^2$ is shown in Fig. 1 for a typical case of $q_x = 0.01$ nm$^{-1}$ and $k_y = 0$ with $M = -6.86$ meV. An almost linear dependence can obviously be seen. Comparing with the single-band Kronig–Penney model, this shows that the bands near the averaged potential are more ground-state like as they are less oscillatory than the bands further away from the averaged potential. It is interesting to point out that when the sign of $M$ changes, the behavior shown in Fig. 1 is qualitatively the same despite the fact that there is no edge state when the system is of a finite size and $M > 0$.

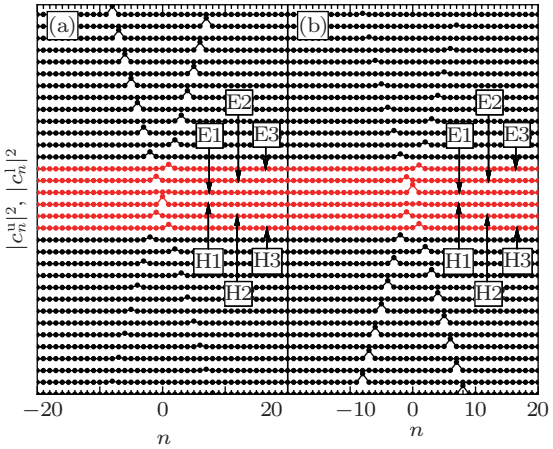



**Fig. 1.** (color online) The square of the Fourier expansion coefficients (a) $|c_n^u|^2$ and (b) $|c_n^l|^2$ of the wave functions for energy levels near the averaged potential $V_0R/L$, where $L = 20$ nm, $q_x = 0.01$ nm$^{-1}$, $k_y = 0$, $V_0 = 0.1$ eV, and $M = -6.86$ meV. The coefficients are shown as dots, and the lines connecting the dots are a guide to the eye. For clarity, the coefficients for different energy levels are shifted vertically in the order of descending energy from the top to the bottom in the figure.

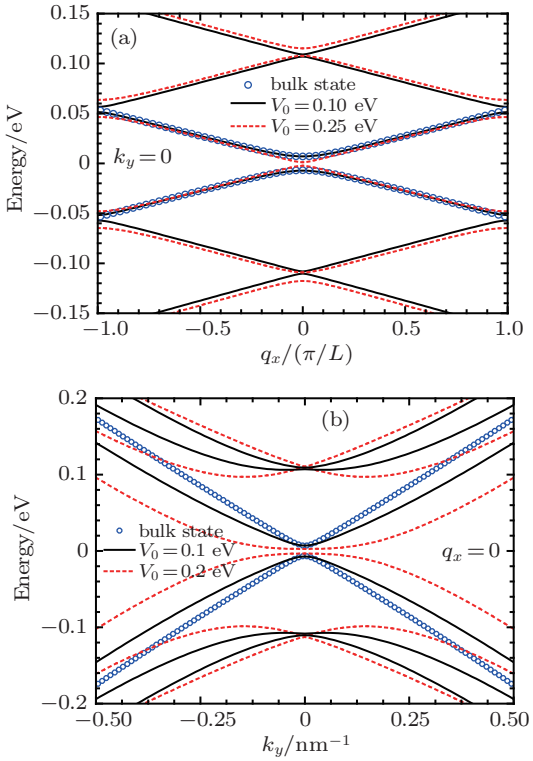



**Fig. 2.** (color online) (a) The energy dispersions along the $q_x$ direction in the first Brillouin zone of the lateral superlattice with $k_y = 0$. The averaged potential energy $V_0R/L$ is subtracted from each energy level. The black solid line is for $V_0 = 0.1$ eV and the red dashed line is for $V_0 = 0.25$ eV. The open circles show the energy dispersion of the bulk states with no shift. (b) The energy levels versus $k_y$ with the averaged potential energy subtracted, and $q_x = 0$. The black solid line is for $V_0 = 0.1$ eV and the red dashed line is for $V_0 = 0.2$ eV. The open circles show the energy dispersion of the bulk states.

In this paper, we assume that the number of electrons in the 2D topological insulator will not be strongly affected by the introduction of the lateral superlattice potential. This approximation is consistent with the assumption of the diagonal addition of the superlattice potential. If the Fermi energy is near the band gap center of the bulk 2D topological insulator, which is taken as the energy zero point, then in the presence of the lateral superlattice potential, the Fermi energy should be close to the averaged potential (the Fermi energy is moved up in the same way as the mini-bands if the carrier density is assumed to be unchanged). Thus in this paper, we will focus on the bands near the averaged potential. For convenience, we label the six bands near the averaged potential as E1, E2, E3, H1, H2, and H3 (see Fig. 1).

In Fig. 2(a), we show the energy dispersion along the $q_x$ direction in the first Brillouin zone ($[-\pi/L, \pi/L]$) for different values of $V_0$ and $k_y = 0$. In Fig. 2(b), the energy dispersion along the $k_y$ direction is shown with $q_x = 0$. In each energy dispersion, the averaged potential energy $V_0R/L$ is subtracted. The bulk bands are also shown in Fig. 2 as open symbols. When $V_0$ is small, bands E1 and H1 are close to the bulk bands, as expected. We wish to point out that when the sign of $M$ is reversed, the energy dispersion is qualitatively unchanged.

The energy dispersion changes in a rather complicated way when the barrier potential $V_0$ changes. In Fig. 3, the six energy levels are shown as a function of $V_0$, with the average potential subtracted, for various values of $q_x$ and fixed $k_y = 0$. One can clearly see that all bands display an oscillatory behavior. There are three critical values of the potential $V_0$ at which bands E1 and H1 (E2 and E3, H2, and H3) touch each other when $q_x = k_y = 0$. The oscillation amplitude is smaller and no touching point exists when $q_x \neq 0$ or $k_y \neq 0$.

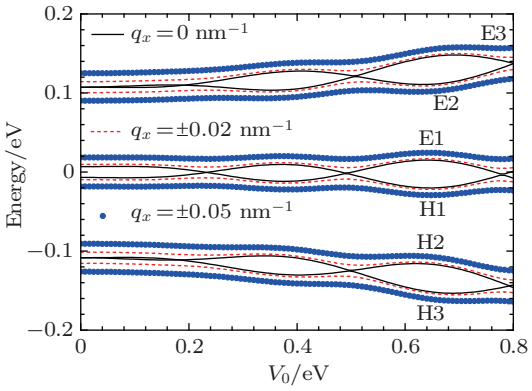



**Fig. 3.** (color online) Energy levels versus the lateral superlattice barrier potential amplitude $V_0$ for various values of $q_x$ and fixed $k_y = 0$. The averaged potential energy is subtracted from each energy level. Curves with opposite signs of $q_x$ are identical.

Next, we study the spatial dependence of the wave functions. The system considered is uniform along the $y$ direction, therefore, we only need to investigate the probability distribution along the $x$ direction. For a specific band, the total distribution can be written as $|\Psi(x)|^2 = |u^u(x)|^2 + |u^l(x)|^2$, with $|u^u(x)|^2$ and $|u^l(x)|^2$ contributed from the upper and the lower components of the corresponding wave function. Figure 4 shows the probability distributions for various values of $q_x$ and $k_y$ with fixed $V_0 = 0.2$ eV. The well/barrier regions are

indicated by two vertical lines. Figures 4(a) and 4(b) are for the E1 band and the H1 band, respectively. It can be seen that, for the E1 band, the amplitude of the wave function in the middle well region ($R/2 < x < L-R/2$) is larger than that in the barrier region ($0 < x < R/2$ and $R/2 < x < L$). For the H1 band, the amplitude of the wave function is larger in the barrier region.

It is interesting to note that the energies of bands E1 and H1 are about 0.1 eV, both below the barrier potential $V_0 = 0.2$ eV. On the other hand, the distribution shows that the E1 band behaves like a state in the well, while the H1 band behaves like a state in the barrier, if we view them in a traditional single band picture. In the single-band case, when the band energy is below the barrier of a superlattice potential, the wave function should be more confined in the well region. The result shown in Fig. 4 indicates that a state whose energy is below the barrier could become localized in the well region or in the barrier region. This resembles the case of the above-barrier states in a semiconductor superlattice.[36–39] This effect is not unexpected, as in the present study, we deal with a two-band model with a strong inter-band coupling.

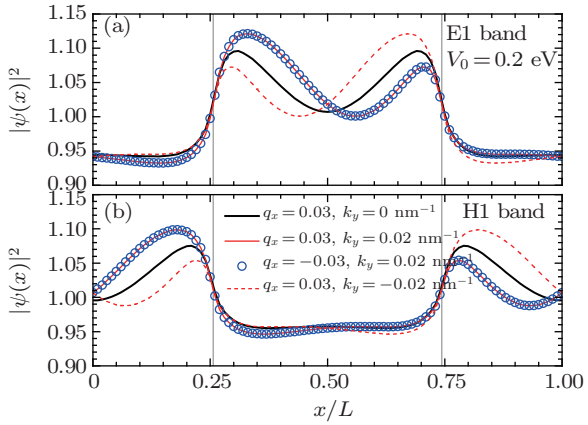



**Fig. 4.** (color online) The spatial dependence of the total wave functions in one lateral superlattice unit cell: (a) the total wave function of the E1 band, (b) that of the H1 band.

As shown in Fig. 4, the electronic states with $k_y = 0$ have a symmetrical distribution about the center of the unit cell $x = L/2$. This symmetry will be destroyed if $k_y \neq 0$. However, the distribution of a state with $k_y = k_y^0 \neq 0$ and the distribution of a state with $k_y = -k_y^0$ are connected by a reflection transformation about the center of the unit cell. By making the reflection transformation, one obtains the distribution for $k_y = -k_y^0$ from that for $k_y = k_y^0$ and vice versa. This symmetry about the distribution is due to the symmetry of the model Hamiltonian, $h^*(k_x, k_y) = h(k_x, -k_y)$.

Next, we study how the probability distribution (the wave function) changes when the lateral superlattice potential $V_0$ changes. This task becomes easier if we introduce the probability distribution integrated over the well region in a unit cell $P_\mathrm{w} = P_\mathrm{w}^\mathrm{u} + P_\mathrm{w}^\mathrm{l}$, where $P_\mathrm{w}^\mathrm{u} = \int_{R/2}^{L-R/2} |u^\mathrm{u}(x)|^2 \mathrm{d}x$ and $P_\mathrm{w}^\mathrm{l} = \int_{R/2}^{L-R/2} |u^\mathrm{l}(x)|^2 \mathrm{d}x$. Similarly, we also introduce $P_\mathrm{b}$, the probability distribution integrated over the barrier region in a unit cell. In Fig. 5, we show the total $P_\mathrm{w}$ for the E1 and H1 bands for various values of $q_x$, $k_y$, and $M$. It is clear that, as the barrier potential $V_0$ increases, the probability distribution in the well displays an oscillatory behavior around the homogenous value 0.5. When $q_x = 0$, the oscillation of $P_\mathrm{w}$ shows abrupt changes at several values of $V_0$ (see Figs. 5(a) and 5(d)). When $q_x \neq 0$, these abrupt changes become smoother.

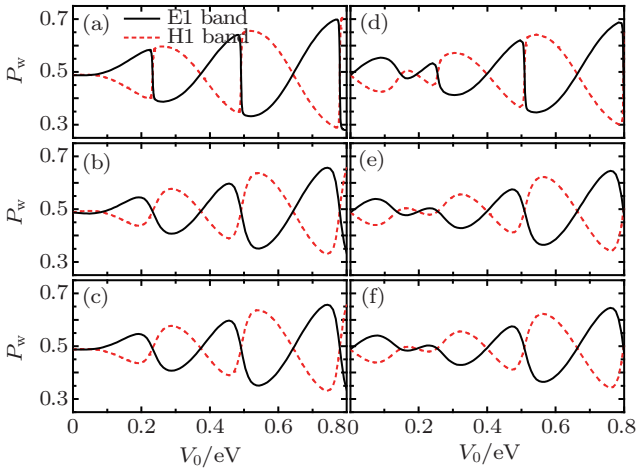



**Fig. 5.** (color online) The wave function integrated in the well region $P_\mathrm{w}$ versus $V_0$ for various values of $q_x$ and $k_y$. The solid curves are for the E1 band and the dashed curves are for the H1 band. In panels (a)–(c), $M = -6.86$ meV; in panels (d)–(f), $M = 6.86$ meV. In panels (a) and (d), $q_x = 0$, $k_y = 0.01\ \mathrm{nm}^{-1}$. In panels (b) and (e), $q_x = 0.01\ \mathrm{nm}^{-1}$, $k_y = 0$. In panels (c) and (f), $q_x = 0.01\ \mathrm{nm}^{-1}$, $k_y = 0.01\ \mathrm{nm}^{-1}$.

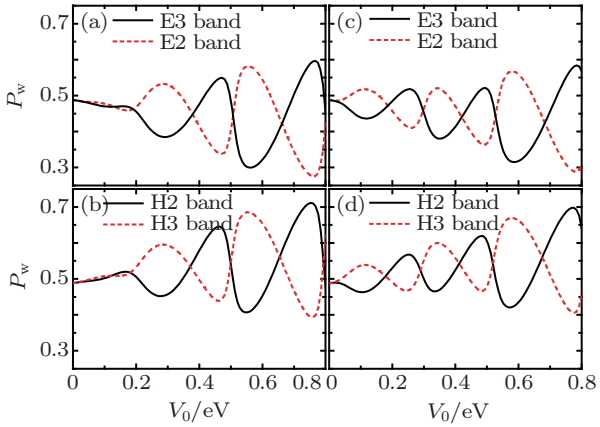



**Fig. 6.** (color online) The wave function integrated in the well region $P_\mathrm{w}$ versus $V_0$ for $q_x = 0.01\ \mathrm{nm}^{-1}$ and $k_y = 0$. Panels (a) and (c) are for E2 and E3 bands, panels (b) and (d) are for H2 and H3 bands, respectively. In panels (a) and (b), $M = -6.86$ meV; in panels (c) and (d), $M = 6.86$ meV.

The integrated probability distributions for E2, E3, H2, and H3 bands are shown in Fig. 6 for $q_x = 0.01\ \mathrm{nm}^{-1}$, $k_y = 0$, and two values of $M$. The oscillatory behavior is similar to that of the E1 and H1 bands except that the oscillation is slightly slantwise to the homogeneous distribution. The states with even higher/lower energies are also investigated and similar results are found. This result is consistent with that in Ref. [22],

where the author found that the spin polarization oscillates across the boundary of a step-function electrical potential on the surface of a three-dimensional topological insulator and is not confined by the potential due to the Klein paradox. By examining Figs. 5 and 6, we observe that the oscillation is not strong, this indicates that the effectiveness of gating on the top of a 2D topological insulator is limited. As we have mentioned, this is due to the coupled two-band nature intrinsic to the system. Moreover, it should be pointed out that the oscillatory pattern can be modified dramatically when a different set of topological insulator parameters[25] is used.

It is well-known that, when the effective model for the 2D topological insulator is applied to a stripe geometry system, the existence of the nontrivial edge states requires that the bulk bands must be inverted, i.e., $M < 0$.[25] When all parameters except $M$ are unchanged, the model with a negative $M$ and that with a positive $M$ have completely different behaviors when applied to the stripe system. In Figs. 5 and 6, we compare $P_{\rm w}$ calculated with a negative $M$ and that with a positive one. The left panels are for the negative $M$ case and the right panels are for the positive $M$ case. In the positive $M$ case, one observes that the number of oscillations increases. However, it is clear that there is no significant difference between the two cases.

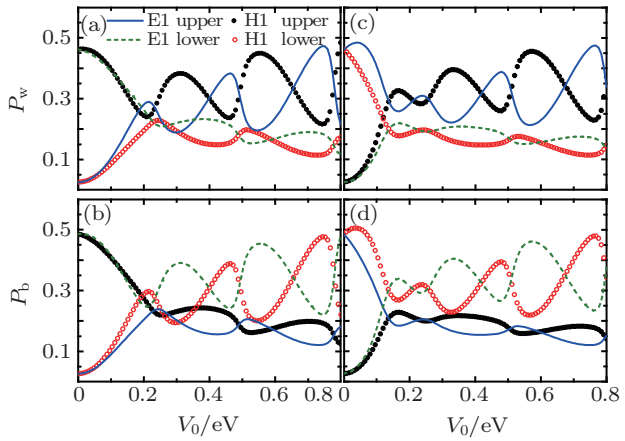



**Fig. 7.** (color online) Panels (a) and (c) show the wave functions integrated in the well region $P_{\rm w}$ versus $V_0$ for the upper and the lower components of the wave function. Panels (b) and (d) show the wave functions integrated in the barrier region versus $V_0$ for both the upper and the lower components. Here $q_x = 0.01$ nm$^{-1}$ and $k_y = 0$. In panels (a) and (b), $M = -6.86$ meV; in panels (c) and (d), $M = 6.86$ meV. The wave functions are shown for bands E1 and H1 only.

As the lateral superlattice studied in this paper is a coupled two-band system, we have evaluated the probability distribution for each component of a state. In Fig. 7, the integrated probability distributions (wave function) are shown for the upper and the lower components of the wave function separately. The integral is performed either inside the potential well region (Figs. 7(a) and 7(c)) or in the barrier region (Figs. 7(b) and 7(d)). Only the results for the E1 and H1 bands are presented. In the left panels, $M < 0$; in the right panels, $M > 0$; $q_x = 0.01$ nm$^{-1}$, and $k_y = 0$. One observes that the two components both display an oscillatory behavior.

In the case of $M < 0$ (Figs. 7(a) and 7(b)), when $V_0$ is small, $P_{\rm w}$ and $P_{\rm b}$ of the H1 band mainly consist of the upper component, and for the E1 band, they are dominated by the lower component. As $V_0$ increases, the difference between the two components becomes small. In contrast, when $M > 0$ (Figs. 7(c) and 7(d)) and $V_0$ is small, the E1 band is mainly contributed by the upper component and the H1 band is dominated by the lower component. More calculations show that when $q_x$ and $k_y$ become large, the contributions to $P_{\rm w}$ and $P_{\rm b}$ from the upper and the lower components will become nearly the same, even in the region of small $V_0$.

## 4. Summary

In summary, we have investigated theoretically the properties of the electronic states of a lateral electrical potential superlattice made of a 2D topological insulator. The dispersion of the mini-band and the electron wave functions in the potential well region are found to display an oscillatory behavior as the potential strength of the lateral superlattice increases. The probability of finding an electron in the potential well region can be larger or smaller than the average as the potential strength varies. These features are different from those in the single-band Kronig–Penney model, and can be attributed to the coupled-multiple-band nature of the 2D topological insulator. Our study suggests that, in a two-dimensional topological insulator, the ability to induce a spatial confinement of electrons via the externally applied electrical gate voltages is not as effective as that in a conventional semiconductor. Thus, in the device design, one should be more careful to manipulate locally the electron density by using an electrical gate.

## References

[1] Zhang S C 2008 *Physics* **1** 6
[2] Qi X L and Zhang S C 2010 *Physics Today* **63** 33
[3] Hasan M Z and Kane C L 2010 *Rev. Mod. Phys.* **82** 3045
[4] Moore J E 2010 *Nature* **464** 194
[5] Yu R, Fang Z and Dai X 2011 *Physics* **40** 462
[6] Ye F and Su G 2010 *Physics* **39** 564
[7] König M, Wiedmann S, Brüne C, Roth A, Buhmann H, Molenkamp L W, Qi X L and Zhang S C 2007 *Science* **318** 766
[8] Hsieh D, Qian D, Wray L, Xia Y, Hor Y S, Cava R J and Hasan M Z 2008 *Nature* **452** 970
[9] Analytis J G, McDonald R D, Riggs S C, Chu J H, Boebinger G S and Fisher I R 2010 *Nat. Phys.* **6** 960
[10] Cheng P, Zhang T, He K, Cheng X, Ma X C and Xue Q K 2011 *Physics* **40** 449
[11] Zhang L B, Chang K, Xie X C, Buhmann H and Molenkamp L W 2010 *New J. Phys.* **12** 083058
[12] Zhang L B, Zhai F and Chang K 2010 *Phys. Rev. B* **81** 235323
[13] Jiang Z F, Chu R L and Shen S Q 2010 *Phys. Rev. B* **81** 115322
[14] Zhang L B, Cheng F, Zhai F and Chang K 2011 *Phys. Rev. B* **83** 081402
[15] Dolcini F 2011 *Phys. Rev. B* **83** 165304
[16] Citro R, Romeo F and Andrei N 2011 *Phys. Rev. B* **84** 161301
[17] Zhang D and Ting C S 2012 *Phys. Rev. B* **85** 115434
[18] Michetti P, Budich J C, Novik E G and Recher P 2012 *Phys. Rev. B* **85** 125309

[19] Wang J, Chen X, Zhu B F and Zhang S C 2012 *Phys. Rev. B* **85** 235131
[20] Romeo F, Citro R, Ferraro D and Sassetti M 2012 *Phys. Rev. B* **86** 165418
[21] Yokoyama T, Balatsky A V and Nagaosa N 2010 *Phys. Rev. Lett.* **104** 246806
[22] Gao J H, Yuan J, Chen W Q, Zhou Y and Zhang F C 2011 *Phys. Rev. Lett.* **106** 057205
[23] Chang K 2011 *Physics* **40** 458
[24] Bernevig B A, Hughes T L and Zhang S C 2006 *Science* **314** 1757
[25] Zhou B, Lu H Z, Chu R L, Shen S Q and Niu Q 2008 *Phys. Rev. Lett.* **101** 246807
[26] Li J, Chu R L, Jain J K and Shen S Q 2009 *Phys. Rev. Lett.* **102** 136806
[27] Chang K and Lou W K 2011 *Phys. Rev. Lett.* **106** 206802
[28] Krueckl V and Richter K 2011 *Phys. Rev. Lett.* **107** 086803
[29] Schmidt M J, Novik E G, Kindermann M and Trauzettel B 2009 *Phys. Rev. B* **79** 241306
[30] Novik E G, Recher P, Hankiewicz E M and Trauzettel B 2010 *Phys. Rev. B* **81** 241303
[31] Krueckl V and Richter K 2012 *Phys. Rev. B* **85** 115433
[32] Takagaki Y 2012 *Phys. Rev. B* **85** 155308
[33] Zhang D, Lou W K, Miao M S, Zhang S C and Chang K 2013 *Phys. Rev. Lett.* **111** 156402
[34] Dombey N and Calogeracos A 1999 *Physics Reports* **315** 41
[35] Masir M R, Vasilopoulos P and Peeters F M 2010 *J. Phys.: Condens. Matter* **22** 465302
[36] Colak S and Shahzad K 1988 *Phys. Rev. B* **38** 9667
[37] Zhang F C, Dai N, Luo H, Samarth N, Dobrowolska M, Furdyna J K and Ram-Mohan L R 1992 *Phys. Rev. Lett.* **68** 3220
[38] Zhang F C, Luo H, Dai N, Samarth N, Dobrowolska M and Furdyna J K 1993 *Phys. Rev. B* **47** 3806
[39] Tseng S M, Chen Y F, Cheng Y T, Hsu C W, Huang Y S and Lin D Y 2001 *Phys. Rev. B* **64** 195311